

Determination of Kinetic Parameters for the Thermal Decomposition of *Parthenium hysterophorus*

Alok DHAUNDIYAL^{1*}, Suraj B. SINGH², Muammel M. HANON^{1,3}, Rekha RAWAT⁴

¹ Mechanical Engineering Doctoral School, Szent istvan University, Godollo 2100, Hungary

² Department of Mathematics, Statistics & Computer Science, Govind Ballabh Pant University of Agriculture and Technology, Pantnagar, U.K., India

³ Baquba Technical Institute, Middle Technical University, Baghdad, Iraq

⁴ School of Agriculture and Forestry, Himgiri Zee University, Dehradun, U.K., India

Abstract – A kinetic study of pyrolysis process of *Parthenium hysterophorus* is carried out by using thermogravimetric analysis (TGA) equipment. The present study investigates the thermal degradation and determination of the kinetic parameters such as activation E and the frequency factor A using model-free methods given by Flynn Wall and Ozawa (FWO), Kissinger-Akahira-Sonuse (KAS) and Kissinger, and model-fitting (Coats Redfern). The results derived from thermal decomposition process demarcate decomposition of *Parthenium hysterophorus* among the three main stages, such as dehydration, active and passive pyrolysis. It is shown through DTG thermograms that the increase in the heating rate caused temperature peaks at maximum weight loss rate to shift towards higher temperature regime. The results are compared with Coats Redfern (Integral method) and experimental results have shown that values of kinetic parameters obtained from model-free methods are in good agreement. Whereas the results obtained through Coats Redfern model at different heating rates are not promising, however, the diffusion models provided the good fitting with the experimental data.

Keywords – Biomass pyrolysis; Coats Redfern method; kinetic parameters; model-free methods; non-isothermal

Nomenclature

E	Activation energy	kJ/mol
A	Frequency factor	s^{-1}
X	Conversion	
t	Time	s
k	Rate constant	
T	Temperature	K
m_0	Initial mass of sample	mg
m_i	Instantaneous mass of sample	mg
m_r	Residual mass of sample	mg
R	Gas constant	(kJ·K)/mol
θ	Heating rate	$^{\circ}\text{C}/\text{min}$
T_m	Peak temperature	$^{\circ}\text{C}$
\bar{T}	Mean temperature	$^{\circ}\text{C}$

*Corresponding author.

E-mail address: Alok.dext@hotmail.com

1. INTRODUCTION

Parthenium hysterophorus, an obnoxious, aggressive Asteraceous weed, has covered over millions of hectares of land in India. This erect, ephemeral weed is known for its prolific growth and high fecundity, especially in the summer season. It is also known as altamisa, carrot grass, bitter weed, star weed, white top, wild feverfew, the 'Scourge of India', and congress grass. It produces thousands of the small white capitula and each of them yields five seeds while reaching its maturity. It has invaded the wilderness of Africa, Asia, Australia and Pacific Islands and has become one of the world's seven most destructive and hazardous weeds. This noxious weed is often noticeable at under developing residential colonies sites, the side of metallic roads, railway tracks, drainage and irrigation canals, etc. The gardens, plantations and vegetable crops are easily overwhelmed by this weed [1]. A single plant can produce around 10 000 to 15 000 viable seeds and these seeds can disseminate and germinate to capture large areas. It is called hazardous as it causes allergic respiratory problems and contact dermatitis in humans and livestock [2], [3]. Productivity of crop is severely affected due to its allelopathy. Invasive species mainly change soil properties, such as moisture, temperature [3], [4], pH [5], [6] and soil organic matters [7]–[9]. Moreover, an aggressive expansion of this weed threatens biodiversity. Elimination of this unwanted weed by burning, chemical herbicides, eucalyptus oil and biological control by leaf feeding beetle, stem-galling moth, stem-boring weevil and fungi have turned out to be successful measures to some extent. However, many innovative uses of this notorious weed have also been discovered. *Parthenium hysterophorus* is utilised to remove heavy metals and dye from the environment, eradication of aquatic weeds, use as substrate for commercial enzyme production, additives in cattle manure for bio-gas production, as biopesticide, as green manure and compost are some of its potential ability.

In this study, *Parthenium hysterophorus* is used to evaluate its untapped thermal potential. As it is mentioned that this weed has a wide range of applications in biochemical, extraction and medical field, is now subjected to thermal decomposition so that its ability as an alternative fuel for thermochemical processes can be assessed. The contribution of bio-waste as an energy reservoir is likely to increase as per the statistics of the European energy policy report [10]. According to the Ministry of New Renewable Energy of India, around 32 % of total primary energy is derived from biomass and more than 70 % of the Indian population relies on it [11]. The total amount of biomass generation per year in India is 546.41 million ton and the major portion of biomass utilization comprises agricultural and forestry residues (around 54 %). Despite the wide application of biomass in the energy sector, there are still some complications which prevail due to the chemical and physical attributes, such as low thermal efficiency as it is highly fibrous, channelling and bridging, and transportation costs [12]. Torrefaction and pelletisation could be useful to solving these problems to some extent. But before proceeding to use a different kind of biomass, it is very essential to have comprehensive knowledge about its chemical and physical behaviour as well as the kinetics of the thermo-chemical process of the biomass.

The objective of this study is to evaluate the kinetics parameters for thermal decomposition of this notorious weed with the help of thermogravimetric analyser (TGA), as this technique is commonly applied for thermal analysis [13], [14]. This analytical method is not only valid for bio-waste but also for thermal decomposition of other materials, such as medical waste [15], waste tyre [16], printed circuit board [17] or sewage sludge [18]. Infestation of arable land is one of the important facets of this work, as in the Karakoram and the Himalayan (Greater, Trans and Lower) ranges of India the percentage of agricultural land is about 10 % in hills, while 90 % is fallow land. This weed

is a kind of a scourge to the hill states of India, so the work encompasses metamorphism and conversion of its side-effect into positive effect for the energy industries of India.

2. MATERIALS AND METHODS

2.1. Material

A sample of weed (*Parthenium hysterophorus*) is investigated to obtain their activation energy (E_x) and pre-exponential factor (A) of Arrhenius equation values for thermal decomposition. The sample of pine needles and *Cedrus deodara* are also considered for comparative analysis with thermograms of weed samples. The chemical composition and higher heating values are obtained with the help of CHNO-S analyser (*Flash EA 1112* series) and Dulong petit formula for calorific value estimation [19]. Table 1 shows chemical composition of *Parthenium hysterophorus* (dry-basis). Those sampled are pre-treated to assure homogeneity and reproducibility of the carried-out tests. The samples are grinded and dried so that ingress of moisture does not affect calculation.

TABLE 1. CHEMICAL COMPOSITION OF
PARTHENIUM HYSTEROPHORUS SAMPLE ON DRY-BASIS

C, %	H, %	N, %	O, %	S, %	H.H.V*, MJ/kg
41.3	5.3	3.3	21.0	0	17.9

* Higher heating value

2.2. TG Method

Each sample of 10.54 mg has undergone thermal decomposition at three different heating rates ($5\text{ }^\circ\text{C min}^{-1}$, $10\text{ }^\circ\text{C min}^{-1}$, $20\text{ }^\circ\text{C min}^{-1}$) in a SII 6300 EXSTAR. A vertical TG/DTG holder is used. To obtain pyrolysis conditions, inert gases are commonly used. In this study, nitrogen atmosphere is used as the purge gas for protecting against possible ingress of pollutants. The volumetric rate is set to 200 mL min^{-1} for the purge gas. Al_2O_3 crucibles are used. To measure the actual sample and furnace temperatures, thermocouple types R is considered.

2.3. Kinetic Models

Kinetic analysis of solid state decomposition is mainly based on a one-step kinetic equation [20]:

$$\frac{dX}{dt} = k(T)f(X), \quad (1)$$

where

$X = \frac{m_0 - m_t}{m_0 - m_r}$ is the extent of conversion;

$f(X)$ represents the reaction model.

The reaction model may be one of them illustrated in Table 2. Here m_0 , m_t and m_r denote initial mass of sample, instantaneous mass and the residual mass respectively. The temperature dependent rate constant $k(T)$ can be replaced by Arrhenius equation, which gives us:

$$\frac{dX}{dt} = A \exp\left(\frac{-E_x}{RT}\right) f(X). \quad (2)$$

The right-hand side of Eq. (2) is also called as kinetic triplet. In case of non-isothermal conditions, the time dependence of conversion is replaced through temperature-time relation (Eq. (3)).

$$\frac{dX}{dT} = \frac{A}{\theta} \exp\left(\frac{-E_X}{RT}\right) f(X), \tag{3}$$

where
 $\theta = \frac{dT}{dt}$ is the heating rate.

TABLE 2. SET OF REACTION MODELS REQUIRED TO DESCRIBE THERMAL DECOMPOSITION IN SOLIDS MODELS

Model No.	Nucleation models	$g(X) = \int_0^X \frac{dX}{f(X)}$
1	Power law	$X^{\frac{1}{4}}$
2	Power law	$X^{\frac{1}{3}}$
3	Power law	$X^{\frac{1}{2}}$
4	Avarami-Erofeev	$[-\ln(1-X)]^{\frac{1}{4}}$
5	Avarami-Erofeev	$[-\ln(1-X)]^{\frac{2}{3}}$
6	Avarami-Erofeev	$[-\ln(1-X)]^{\frac{1}{2}}$
Diffusion models		
7	1-dimensional diffusion	X^2
8	Diffusion control	$\left(1 - (1-X)^{\frac{1}{3}}\right)^2$
Reaction order and geometrical contraction models		
9	Mampel (first order)	$-\ln(1-X)$
10	Second order	$(1-X)^{-1} - 1$
11	Contracting Cylinder	$1 - (1-X)^{\frac{1}{2}}$
12	Contracting Sphere	$1 - (1-X)^{\frac{1}{3}}$

There are two different mathematical schemes to evaluate kinetic parameters for thermal decomposition of biomass samples. The first one is model-free methods (iso-conversional technique), whereas the second approach is known as model based methods as it depends upon the different reaction models given in Table 2.

After rearrangement of Eq. (3), we have:

$$g(X) = \int_0^X \frac{dX}{f(X)} = \int_{T_0}^T \frac{A}{\theta} \exp\left(\frac{-E}{RT}\right) dT. \tag{4}$$

Eq. (4) can also be rewritten as:

$$g(X) = \int_0^X \frac{dX}{f(X)} = \frac{AE_a}{R\theta} I\left(\frac{E_a}{RT}\right). \quad (5)$$

The term $\left(\frac{E_a}{RT}\right)$ has no exact solution and it must be solved by the numerical approximations as in literature [14].

2.3.1. Model-Free Methods

The model-free methods are based on evaluating the Arrhenius parameters without relying upon the reaction order [21], [22]. Model-free method is also called isoconversional, as the reaction rate is a function of the temperature at constant extent of conversion [23]. Isoconversional methods are valid to analyse both isothermal and non-isothermal pyrolysis. In the 1960s, various isoconversional methods were proposed [24]–[26]. These methods involve the series of experiments performed at different heating rates.

2.3.1.1. Kissinger Method

The ASTM E698 method [27] shared a different perspective which lies between the model-based and model-free methods. Unlike other isoconversional models, there is no need to estimate E_a for each conversion value. It takes a model-free approach for estimation of activation energy which is evaluated from Kissinger’s plot of $\ln\left(\frac{\theta}{T_m^2}\right)$ against $\left(\frac{1}{T_m}\right)$ [28], where T_m is the temperature corresponding to the maximum of $\frac{dX}{dT}$. However, for both the non-isothermal and isothermal pyrolysis, pre-exponential factor is calculated on the assumption of first-order reaction as follows:

$$A = \frac{\theta E}{RT_m^2} \exp\left(\frac{E}{RT_m}\right). \quad (6)$$

The following equation is considered:

$$\ln\left(\frac{\theta}{T_m^2}\right) = \ln\left(\frac{AR}{E_X}\right) - \frac{E_X}{RT_m}. \quad (7)$$

Here, activation energy is estimated as a slope of the plot, which is equal to $\frac{-E_a}{R}$.

The value of T_m can be computed from derivative of conversion (X) over Temperature (T) (illustrated in Fig. 4).

2.3.1.2. Flynn-Wall-Ozawa Method

The solution of Eq. (5) using Doyle’s approximations (Eq. (8)) [29] provides the Flynn-Wall-Ozawa (FWO) method (Eq. (9)) [25], [26]:

$$I\left(\frac{E_X}{RT}\right) \cong -5.331 - 1.052 \frac{E_X}{RT}, \quad (8)$$

$$\ln(\theta_i) = \ln\left(\frac{AE_{X_i}}{Rg(X_i)}\right) - 5.331 - 1.052 \frac{E_{X_i}}{RT}. \quad (9)$$

Eq. (8) is valid only if $20 \leq \frac{E_a}{RT} \leq 60$ [25].

Here subscript ‘ X_i ’ represents a fixed conversion with different heating rates. The plot of Eq. (9) is a straight line with the slope $-1.052 \frac{E_{X_i}}{RT}$.

2.3.1.3. Kissinger-Akahira-Sunose

The Kissinger-Akahira-Sunose method (KAS) is derived by using approximation for $I\left(\frac{E_a}{RT}\right)$ (Eq. (10)), which is valid within interval of $20 \leq \frac{E_a}{RT} \leq 50$ [30]:

$$I\left(\frac{E_X}{RT}\right) \cong \frac{\exp\left(\frac{-E_X}{RT}\right)}{\left(\frac{E_X}{RT}\right)^2}. \quad (10)$$

In this method, the relation between the temperature and the heating rate is given by Eq. (11) [28]:

$$\ln\left(\frac{\theta_i}{T_{X_i}^2}\right) = \ln\left(\frac{A_X R}{g(X)E_X}\right) - \frac{E_X}{RT_{X_i}}. \quad (11)$$

The apparent activation energy can be estimated from a plot drawn between $\ln\left(\frac{\theta_i}{T_{X_i}^2}\right)$ versus $\frac{1000}{T_{X_i}}$ for a fixed value of conversion X , where the slope is equal to $-\frac{E_X}{R}$.

2.3.2. Model-Based Methods (Coats-Redfern Method)

Coats-Redfern applied the asymptotic technique for approximating the exponential integral in Eq. (5) [31]:

$$\ln\left(\frac{g(X)}{T^2}\right) = \ln\left(\frac{AR}{\theta E_X}\left(1 - \frac{2RT}{E_X}\right)\right) - \frac{E_X}{RT}. \quad (12)$$

If the term $\frac{2R\bar{T}}{E_X}$ is less than one, it can be ignored, and the right-hand side becomes constant.

Here \bar{T} is the mean experimental temperature.

After plotting $\ln\left(\frac{g(X)}{T^2}\right)$ against $\frac{1}{T}$, E_X and A are obtained from slope and intercept respectively. However, it is to be checked for each model provided in Table 2. The model which provides the best fitting is selected as the chosen model. With the help of this model, a kinetic triplet can be evaluated from thermo-analytical data [32]. The value obtained for different reaction regimes at different heating rate is illustrated in Table 2.

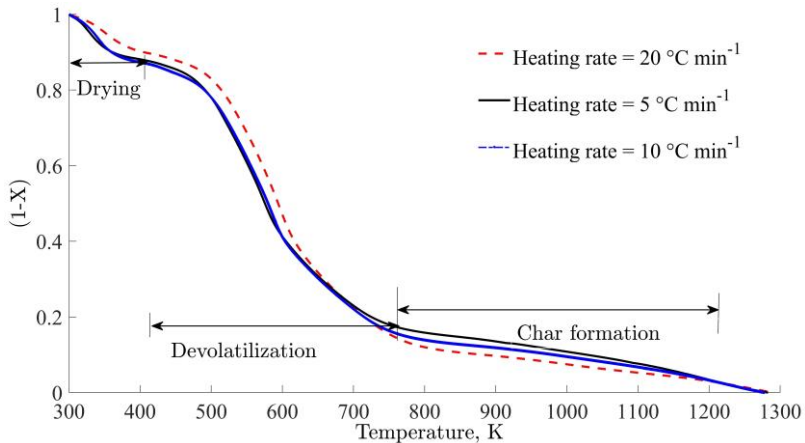
3. RESULTS AND DISCUSSIONS

3.1. Material Characteristic

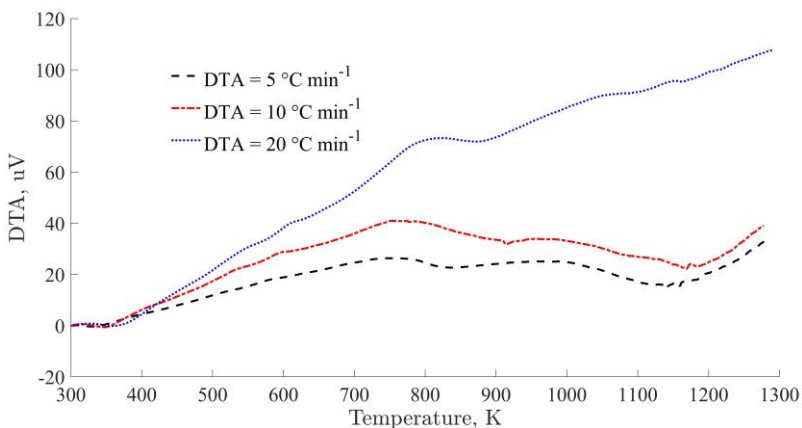
Unlike other forestry biomass [12], *Parthenium hysterophorus* contains a lesser percentage of carbon and hydrogen, therefore it has low higher heating value. This is due to the fact that energy content of carbon-carbon bond is higher than that of carbon-oxygen and carbon-hydrogen bonds. Through analytical chromatography of this weed, as depicted in Table 1, it has been observed that the percentage of sulphur and nitrogen is lower than another loose biomass used [12]. Therefore, it resulted in low greenhouse gas emissions. The gross calorific value of this weed is found to be 17.92 MJ/kg.

3.2. Thermal Analysis

Assessment of *Parthenium hysterophorus* is carried out with the help of thermogravimetric (TG) and differential thermogravimetric (DTG) at three heating rates of $5\text{ }^{\circ}\text{C min}^{-1}$, $10\text{ }^{\circ}\text{C min}^{-1}$ and $20\text{ }^{\circ}\text{C min}^{-1}$ in a nitrogen atmosphere. The DTG curve is basically the first order derivative of TGA curve with respect to time or temperature. It depicts peak temperature at which maximum decomposition occurs in the TGA curves. The TG curves show the fraction of mass loss take place over a range of 300.82 K to 1300 K. It is clearly indicated from Fig. 1 that the most of volatile fraction is released within an interval of 400 K to 800 K. Pyrolysis of weed is divided into three different regimes, such as drying, devolatilization and char formation. The initial temperature for all the TGA experiments is fixed to be 300.82 K. Expelling out of moisture is accomplished in the temperature range of 300.82 K to 400 K. The devolatilization regime begins with formation of tar and volatile gases (CO , CO_2 and heavy hydro carbons) at 400 K and it lasts till 800 K. Further increase in the temperature led to conversion of the weed into solid, black residue (charcoal) char with the drastic falling off the content of volatile content.



(a)



(b)

Fig. 1. TG and DTA of *Parthenium hysterophorus* at different heating rates (a –TG; b –DTA).

Dhaundiya, et al. [33] reported that the major devolatilization occurs in the range of 550 K to 670 K, which is termed as the region of active pyrolysis in Fig. 2 and Fig. 4, while the region at which the decomposition rate is the lowest is demarcated as region of passive pyrolysis in Fig. 2 and Fig. 4. In this region devolatilization ceases to act, that is the regime of char formation is initiated, thus obtained carbon and ash as the final solid residue. It is clearly noticeable at onset of char formation regime, there is an iota of increase in the mass of sample which is owing to cumulative increase in the char formation through simultaneous decomposition of lignin and hemicellulose, and as matter of fact, at end of devolatilization regime, volatile gases recombine with solid material, thus triggering autocatalytic secondary reactions. In Fig. 1(b) there is a drastic variation of change of temperature of *Parthenium hysterophorus* with respect to reference material as it shows anomaly from similar kind of biomass, as after 800 K the nature of reaction becomes exothermic with increase in the heating rate. However, the nature of reaction depends on the direction of heat fluxes relative to the grain orientation of sample and increases the residence time of pyrolysis gases, which in turn triggers the secondary reactions.

The range of temperature from 410 K to 525 K representing the zone of decomposition of hemicellulose at low heating rate, while it is 430 K to 535 K for high heating rate. The first local maximum in Fig. 2 (local minimum in Fig. 4) corresponds to the time or temperature at which the maximum rate of decomposition of hemicellulose takes place. The global maximum (global minimum in Fig. 4) within given range of temperature indicates temperature at which the maximum decomposition rate of cellulose occurred varies from 575 K to 598 K. Degradation of lignin begins after 600 K and it keeps decomposition until it does not reach the final pyrolysis temperature of 1273 K, however decomposition of lignin takes places in both regions of active and passive pyrolysis without any characteristic peaks and it is difficult to distinguish from decomposition of cellulose and hemicellulose.

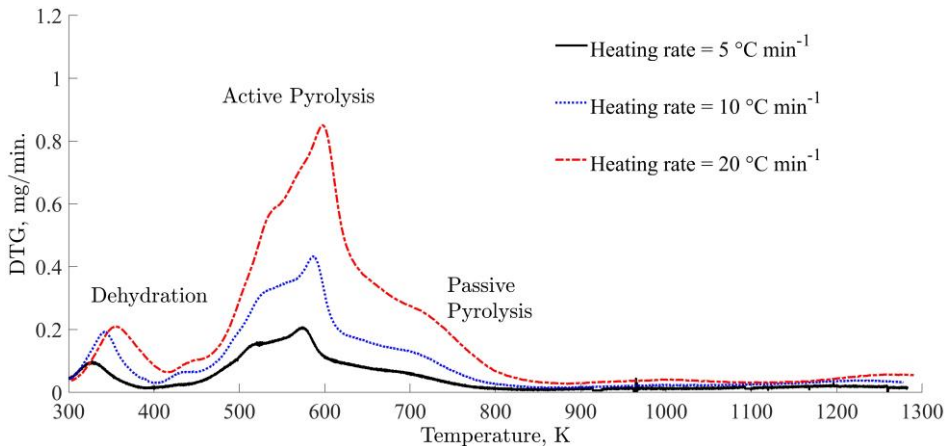


Fig. 2. DTG of *Parthenium hysterophorus* sample observed in the presence of nitrogen at different heating rates. Different stages are: dehydration, active and passive pyrolysis.

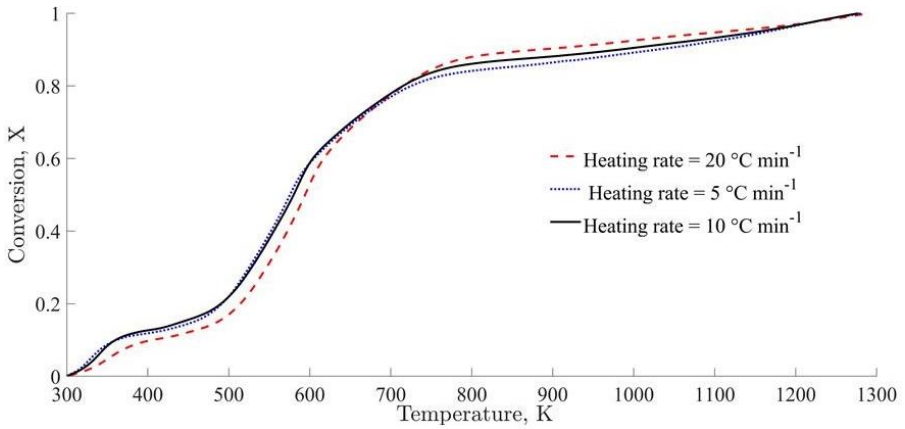


Fig. 3. Extent of conversion curves for the pyrolysis process of pine needles at different heating rate.

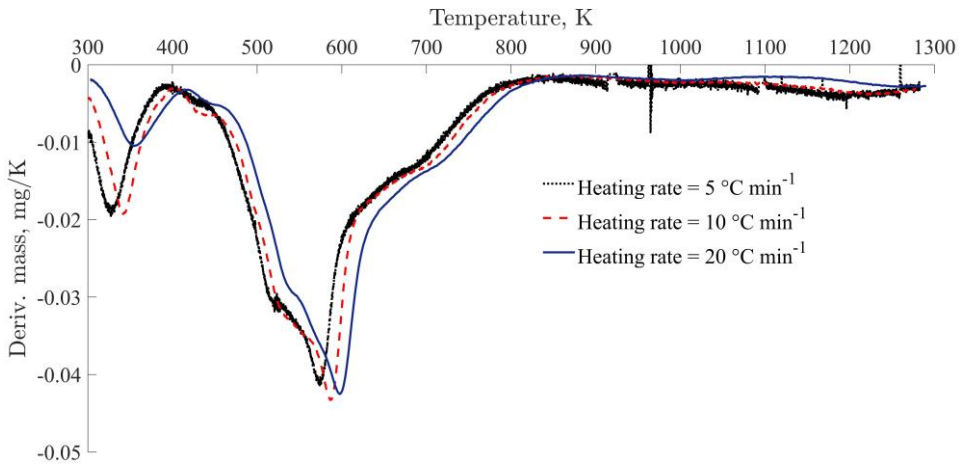


Fig. 4. DTG curves of *Parthenium hysterophorus* with respect to temperature at different heating rates.

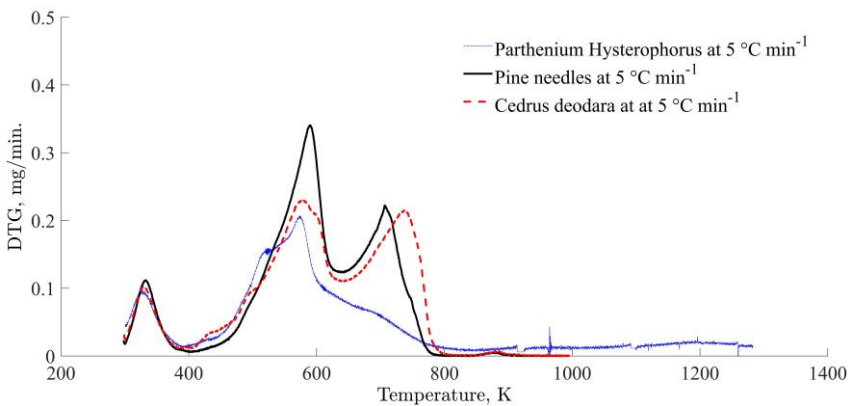


Fig. 5. Comparison of DTG curves of mass fraction as functions of temperature of coniferous species with *Parthenium hysterophorus* at heating rate of $5\text{ }^{\circ}\text{C min}^{-1}$.

The peak complexity is more visible at higher heating rates due to relatively high content of hemicelluloses decomposes at lower temperature than cellulose. The mass loss rate of cellulose significantly increases with temperature [34] and reached its maximum value at about 600 K, while it is 520 K and 710 K for hemicellulose and lignin respectively. The reason of shifting of the global minimum and the local minimum towards higher temperature regime within the same time interval is due to limitation of heat transfer, as at low heating rate a large instantaneous thermal energy is provided to the system and appreciable time is taken by purge gas, nitrogen, to attain equilibrium with the temperature of the sample. On the contrary, the same time scale has been reduced at high heating rate, thus reaction time decreases. Hence, at the same instant of time, temperature required to decompose the sample is also increased [35], [36]. This data is correlated with similar kinds of loose biomasses, pine needles and *Cedrus deodara* leaves and it validates that there is no shift in the global maximum at the same heating rate, as depicted in Fig. 5. The fine sample powder is used for analysis, therefore the thermal gradient between the furnace and the sample is negligibly small. The size and its contact with pan may affect its thermal stability and decomposition temperature. However, the larger size increases its sensitivity, but transition becomes sharp and causes spurious peaks as biomass heated. Thermal decomposition temperature increases as the particle size decreases and increase in heating rate [37].

3.3. Determination of Kinetic Parameters

Estimation of kinetic parameters involves activation energy, and pre-exponential factor of the weed. The sample of weed has undergone non-isothermal temperature history in the presence of nitrogen Atmosphere. This study proposes different model-free methods and comparison of them with the integral method, i.e. Model based method (Coats-Redfern). Kissinger, FWO, KAS and Coats-Redfern methods are used to determine kinetic parameters. Pyrolysis of the weeds is demarcated by three different regions and kinetic analysis of each region is separately assessed. In the first method, the activation energy and pre-exponential factor is estimated with the help of Eq. (7), where T_m indicates an onset temperature corresponding to the maximum mass loss peaks. The peak temperatures are derived from Fig. 4. The benefit of using the model-free method is non-forcible fitting of reaction model to prevailing problem. Kinetic parameters obtained from model-free method can be easily obtained without any presumption on reaction scheme.

3.3.1. Kinetic Parameters Derived from Kissinger Method

Kissinger method is model-free but not isoconversional, as the degree of conversion at the peak temperature (T_m) is constant at different heating rates, therefore provides a single set value of kinetic parameters for the whole process, but it is difficult to assess the complexity of reaction mechanism through this methodology [38].

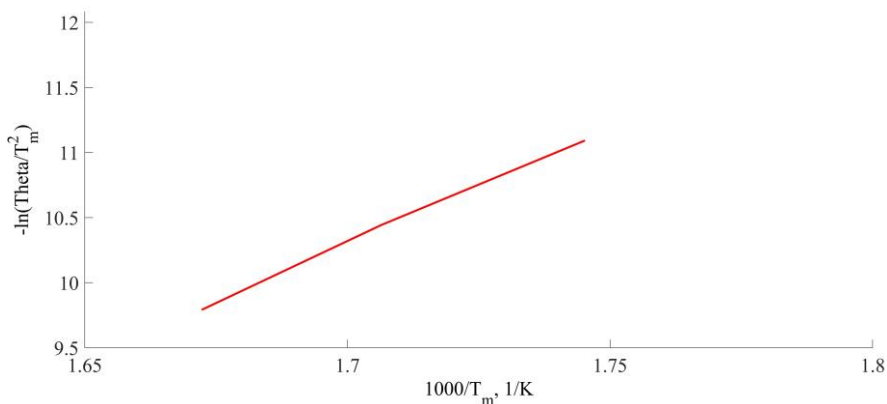


Fig. 6. Kissinger plot of *Parthenium hysterophorus*.

The slope and intercept are computed by plotting linear regression lines between $\ln\left(\frac{\theta}{T_m^2}\right)$ and $\frac{1}{T_m}\left(\frac{1}{K}\right)$, as shown in Fig. 6. Furthermore, $148.047 \text{ kJ/mol}^{-1}$ and $8.38 \cdot 10^{13} \text{ min}^{-1}$ are estimated as activation energy and pre-exponential factor respectively.

3.3.2. Kinetic Parameters Derived from FWO and KAS

The kinetic parameters estimated from FWO and KAS methods are calculated at different values of conversion from Eq. (9) and Eq. (11) respectively. Variation in the conversion (X) at different heating rate with respect to temperature is shown in Fig. 3. To evaluate the kinetic parameters, the same value of conversion (X) is chosen for FWO and KAS with the corresponding temperatures at different heating rates. The comprehensive details of kinetic parameters along with coefficient of regression (R^2) at different degree of conversion are summarized in Table 3. The plot of apparent activation energies, obtained at the same conversion from FWO and KAS, is plotted against conversion, as shown in Fig. 7. It has been found that the apparent activation energy is a function of fractional conversion, as the most of pyrolysis reaction does not follow single step reaction and they rely on multi-step reaction which can also be recognized from Fig. 7 that apparent activation energies calculated from FWO and KAS at different conversion are not similar and exhibits the existence of complex multi-reaction mechanism within the solid matrix. The averaged activation energies and pre-exponential factors calculated from FWO and KAS are 145.81 kJ/mol and 145.44 kJ/mol , $4.77 \cdot 10^{24} \text{ kJ/mol}$ and $3.16 \cdot 10^{24} \text{ kJ/mol}$ respectively. The value of activation energy derived from Kissinger method (148.07 kJ/mol) is consistent with the values of activation energies derived from FWO and KAS. It is also at proximity of average values obtained from them. The value the pre-exponential factor is also in the domain of average values computed from FWO and KAS. However, the influence of ambient atmosphere used in TG analysis effect the computation of kinetic parameters, as Kumar, et al. [39] reported that the activation energy estimated in air is higher than E_a in nitrogen atmosphere, therefore it becomes indispensable to examine the thermochemical process in the presence of inert atmosphere. For a similar kind of loose biomass, Dhaundiya and Tewari [33] examined the thermal degradation of a similar kind of loose biomass by TG/DTA and applied multi reaction model to each constitutes species of biomass and they have found 152.0527 kJ/mol for the cellulose and 133.549 kJ/mol for hemicelluloses, which is found to be consistent with model-free methods. For comparative

evaluation of weed from another integral method than DAEM, Coats Redfern method is adopted to identify the reaction scheme suits to decomposition of weed.

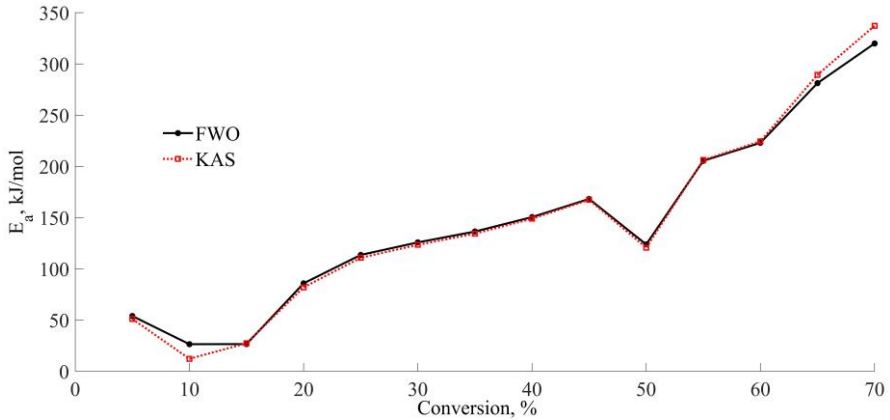


Fig. 7. Activation energy as a function of conversion.

Using simple numerical approximation, Cai and Liu [40] reported that 300 kJ/mol could be as activation energy for thermal decomposition of peanut-shell. In another experiment, Dhaundiya and Singh [41] conducted experiments on *Cedrus deodara* leaves and estimated 39 kJ/mol as an activation energy for it. Lim and his co-worker [42] evaluated the averaged activation energy of 51.19 kJ/mol for rice husk using Kissinger-Akahira-Sunrose (KAS).

TABLE 3. KINETIC PARAMETERS OBTAINED BY MODEL-FREE METHODS

Conversion (X_i)	FWO			KAS		
	E_a , kJ/mol	A , min ⁻¹	R^2	E_a , kJ/mol	A , min ⁻¹	R^2
0.05	53.99	$9.40 \cdot 10^6$	0.92	51.13	$2.11 \cdot 10^6$	0.99
0.10	26.51	$5.31 \cdot 10^3$	0.72	12.26	$3.30 \cdot 10^4$	0.99
0.15	26.62	$2.14 \cdot 10^2$	0.99	27.50	$8.70 \cdot 10^3$	0.60
0.20	85.92	$1.32 \cdot 10^8$	0.80	82.04	$3.50 \cdot 10^7$	0.80
0.25	113.62	$4.94 \cdot 10^{10}$	0.81	110.86	$2.16 \cdot 10^{10}$	0.80
0.30	125.86	$4.60 \cdot 10^{11}$	0.87	123.49	$2.35 \cdot 10^{11}$	0.84
0.35	136.46	$2.78 \cdot 10^{12}$	0.87	134.42	$1.59 \cdot 10^{12}$	0.86
0.40	150.53	$3.47 \cdot 10^{13}$	0.88	149.00	$2.32 \cdot 10^{13}$	0.86
0.45	168.27	$1.07 \cdot 10^{14}$	0.90	167.46	$7.20 \cdot 10^{14}$	0.90
0.50	123.89	$5.48 \cdot 10^{10}$	0.99	120.71	$2.30 \cdot 10^{10}$	0.99
0.55	205.47	$6.80 \cdot 10^{17}$	0.88	206.23	$7.68 \cdot 10^{17}$	0.88
0.60	223.00	$1.14 \cdot 10^{18}$	0.70	224.43	$1.21 \cdot 10^{19}$	0.70
0.65	281.28	$2.29 \cdot 10^{23}$	0.71	289.41	$4.44 \cdot 10^{23}$	0.70
0.70	320.00	$6.65 \cdot 10^{25}$	1.00	337.24	$4.37 \cdot 10^{25}$	0.70
Average	145.81	$4.77 \cdot 10^{24}$		145.4414	$3.16 \cdot 10^{24}$	
Kissinger		148.047 kJ/mol			$8.38 \cdot 10^{23}$ min ⁻¹	

3.3.3. Kinetic Parameters Obtained from the Model-Based Method

The Coats Redfern Eq. (12) is adopted to assess validity of model-free method and provide the most suitable reaction model for decomposition of weed. This model-based method relies on Arrhenius equation. Unlike model-free methods which are based on the degree of conversion, the Coats Redfern depends only on heating rates. Table 2 summarized different kinetic models which are tested to identify the reaction mechanism of pyrolysis of weed. Table 4 illustrates the kinetic parameters for weed evaluated from model based method at different heating rates. It can be observed that kinetic parameters computed at different heating rate for models has shown an appreciable variation from the model-free method, however, the diffusion mechanism has significantly influence the thermo-analytical data than that of the other reaction mechanisms. There are two main reasons for inconsistency between model-free and model based in case of non-isothermal runs. The first is a result of the force-fitting of non-isothermal data to hypothetical reaction model. Arrhenius parameters are determined by form of $g(X)$, which is already assumed. Moreover, both temperature and the conversion (X) are simultaneously varying with time. The model-based model is not able to distinguish separately temperature dependence of rate constant and the conversion. Consequently, any assumed model can be easily synchronised with thermoanalytical data at the expense of drastic variation between the assumed model and the true unknown model. Owing to this reason, the model based methods provide ambiguous values of Arrhenius parameters. Another main reason of disagreement is the existence of multi-reaction mechanisms with different activation energies, as contribution of these steps to the overall decomposition rate is influenced by temperature and extent of conversion, which implies activation energy calculated from the model based method is a function of T and X . However, the calculated value of activation energy represents the average value for the overall process. This value is derived in such a way that it is invariant to the reaction mechanism and kinetics with change in temperature and degree of conversion, therefore, the isoconversional method is prefer to the model based scheme to overcome afore mentioned drawbacks [25], [26], as these models checks dependency of data with respect to conversion or temperature without prior judgement about assumed model.

TABLE 4. KINETIC PARAMETERS OBTAINED BY MEANS OF COATS-REDFERN METHOD

Heating rate (non-isothermal)									
5 °C min ⁻¹				10 °C min ⁻¹			20 °C min ⁻¹		
Model No	E_a , kJ/mol	A , min ⁻¹	R^2	E_a , kJ/mol	A , min ⁻¹	R^2	E_a , kJ/mol	A , min ⁻¹	R^2
1	7.13	$9.80 \cdot 10^9$	0.86	6.71	$1.73 \cdot 10^{10}$	0.83	5.98	$2.81 \cdot 10^{10}$	0.79
2	6.13	$7.50 \cdot 10^9$	0.80	5.63	$1.26 \cdot 10^{10}$	0.73	4.70	$1.88 \cdot 10^{10}$	0.64
3	4.13	$3.97 \cdot 10^9$	0.54	3.46	$5.99 \cdot 10^9$	0.41	2.14	$6.22 \cdot 10^9$	0.19
4	5.83	$5.38 \cdot 10^9$	0.82	3.21	$1.44 \cdot 10^9$	0.21	4.65	$1.44 \cdot 10^{10}$	0.76
5	1.33	$3.46 \cdot 10^8$	0.64	5.42	$6.86 \cdot 10^8$	0.81	3.96	$2.74 \cdot 10^9$	0.47
6	1.53	$6.64 \cdot 10^8$	0.64	0.89	$9.34 \cdot 10^9$	0.06	0.51	$6.47 \cdot 10^8$	0.02
7	14.00	$1.54 \cdot 10^9$	0.83	16.00	$2.51 \cdot 10^9$	0.65	21.00	$3.45 \cdot 10^9$	0.74
8	20.05	$2.91 \cdot 10^9$	0.83	43.29	$1.34 \cdot 10^{16}$	0.85	27.21	$5.42 \cdot 10^9$	0.86
9	7.07	$6.67 \cdot 10^9$	0.68	8.16	$1.26 \cdot 10^9$	0.70	10.86	$2.27 \cdot 10^9$	0.79
10	16.00	$1.14 \cdot 10^9$	0.92	17.00	$1.94 \cdot 10^8$	0.86	19.93	$2.63 \cdot 10^8$	0.91
11	7.40	$1.10 \cdot 10^{10}$	0.82	5.18	$4.03 \cdot 10^9$	0.41	7.77	$8.52 \cdot 10^9$	0.59
12	8.50	$1.43 \cdot 10^{10}$	0.95	6.07	$5.35 \cdot 10^9$	0.51	8.69	$1.06 \cdot 10^{10}$	0.66

4. CONCLUSION

Thermal and kinetic behaviour of weed is investigated through thermogravimetric analysis performed at non-isothermal condition. Activation energy and pre-exponential factor are determined with the help of model-free and model-based methods. The activation energies estimated from Kissinger method is 148.047 kJ/mol, whereas the average values of activation energy derived from FWO and KAS are 145.81 kJ/mol and 145.44 kJ/mol respectively. The values obtained from FWO and KAS are consistent with Kissinger method, however, the values estimated with the help of the Coats-Redfern at different heating rates have shown an appreciable deviation from the expected values estimated from model-free methods. Moreover, apparent values of activation energies at different conversion have indicated the existence of the multi-reaction scheme. The inability of the model based method to correlate with the isoconversional methods is unable to demarcate variation of temperature and degree of conversion with respect to time. The results are also in good agreement with other literature works for similar sort of loose biomass.

Results furnish the significant thermal decomposition details about a weed that can be useful for developing pyrolysis plant and to comprehend mechanism of biomasses that come under purview of low bulk density biomass. In context of bulk density, this weed is relatively like pine needles, but the behavior is quite different. The release of energy per unit mass is more than that of pine needles at the same temperature. The nature of reaction is exothermic with increase in the heating rate as time proceeds, whereas it is mostly endothermic in different kind of biomass like wood, pine needles and *Cedrus deodara* leaves. It shows that residence time of volatile gases is relatively higher than the similar kind of forestry biomass and leads to increase in secondary pyrolysis reactions. This biomass can possibly be a good primary fuel for biofuel production. Temperature required for decomposition of the weed has a negative offset of 1 °C to 2 °C. While gasifying a biomass in a gasifier plant, the temperature required for drying the biomass is to be kept low, so that the heat loss can be minimised during computation of efficiency of gasifier plant. This weed needs less heat content as compare to other similar kind of forestry waste. Heat required for thermal decomposition may reduce the energy consumption for getting the same output. Exergy analysis of gasification process of this weed may provide a noteworthy outcome in context of plant modelling.

ACKNOWLEDGMENT

This work was supported by the Stipendium Hungaricum Programme and by the Mechanical Engineering Doctoral School, Szent Istvan University, Godollo, Hungary.

REFERENCES

- [1] Raghubanshi A. S., Rai L., Gaur J. P., Shing J. S. Invasive al species and biodiversity in India. *Curr. Sci. India*. 2005;88(2):539–540.
- [2] Evans H. C. *Parthenium hysterophorus*, a review of its weed status and the possibilities for biological control. *Biocontrol News and Information* 1997;18(3):89N–98N.
- [3] Levine J. M., Vila M., D'Antonio C. M., Dukes J. S., Grigulis K., Lavorel S. Mechanisms underlying the impacts of exotic plant invasions. *Proc. R. Soc. B* 2003;270:775–781. [doi:10.1098/rspb.2003.2327](https://doi.org/10.1098/rspb.2003.2327)
- [4] Belnap J., Phillips S. L. Soil biota in an ungrazed grassland: Response to annual grass (*Bromus tectorum*) invasion. *Ecol. Appl.* 2001;11(5):1261–1275. [doi:10.2307/3060918](https://doi.org/10.2307/3060918)
- [5] Zavaleta E. Valuing ecosystem services lost to Tamarix invasion in the United States. *Invasive Species in a Changing World*. Washington: Island Press, 2000.

- [6] D'Antonio C. M. Mechanisms controlling invasion of costal plant communities by the alien succulent *Carpobrotus edulis*. *Ecology* 1993;74(1):83–95. doi:10.2307/1939503
- [7] Kourtev P. S., Ehrenfeld J. G., Huang W. Z. Effects of exotic plant species on soil properties in hardwood forests of New Jersey. *Water, Air, and Soil Pollution* 1998;105:493–501. doi:10.1023/A:1005037105499
- [8] Dassonville N., Vanderhoeven S., Vanparys V., Hayez M., Gruber W., Meerts P. Impacts of alien invasive plants on soil nutrients are correlated with initial site conditions in NW Europe. *Oecologia* 2008;157:131–140. doi:10.1007/s00442-008-1054-6
- [9] Ehrenfeld J. G. Effects of exotic plant invasions on soil nutrient cycling processes. *Ecosystems* 2003;6:503–523. doi:10.1007/s10021-002-0151-3
- [10] European Environment Agency (EEA). Europe 2020: a strategy for smart, sustainable and inclusive growth 2010.
- [11] Ministry of New Renewable Energy. Biomass power and cogeneration programme, 2012. Available: <http://mnre.gov.in/schemes/grid-connected/biomass-powercogen>
- [12] Dhaundiya A., Gupta V. K. The analysis of pine needles as a substrate for gasification. *J. Water, Energy Environ.* 2014;15:73–81. doi:10.3126/hn.v15i0.11299
- [13] Di Blasi C. Combustion and gasification rates of lignocellulosic chars. *Progress in Energy and Combustion Science* 2009;35(2):121–140. doi:10.1016/j.peccs.2008.08.001
- [14] White J. E., Catallo W. J., Legendre B. L. Biomass pyrolysis kinetics: A comparative critical review with relevant agricultural residue case studies. *Journal of Analytical and Applied Pyrolysis* 2011;91(1):1–33. doi:10.1016/j.jaap.2011.01.004
- [15] Zhu H. M., Yan J. H., Jiang X. G., Lai Y. E., Cen K. F. Study on pyrolysis of typical medical waste materials by using TG-FTIR analysis. *Journal of Hazardous Materials* 2008;153:670–676. doi:10.1016/j.jhazmat.2007.09.011
- [16] Koreoova Z., Juma M., Annus J., Markos J., Jelemensky L. Kinetics of pyrolysis and properties of carbon black from a scrap tire. *Chemical Papers* 2006;60(6):422–426. doi:10.2478/s11696-006-0077-x
- [17] Quan C., Li A., Gao N. Thermogravimetric analysis and kinetic study on large particles of printed circuit board wastes. *Waste Management* 2009;29(8):2353–2360. doi:10.1016/j.wasman.2009.03.020
- [18] Folgueras M. B., Diaz R. M., Xiberta J., Prieto I. Thermogravimetric analysis of the co-combustion of coal and sewage sludge. *Fuel* 2003;82:2051–2055. doi:10.1016/S0016-2361(03)00161-3
- [19] Mason D., Gandhi K. Formulas for calculating the calorific value of coal and coal chars: Development, tests, and uses. *Fuel Processing Technology* 1983;7(1):11–22. doi:10.1016/0378-3820(83)90022-X
- [20] Brown M., Dollimore D., Galwey A. K. Reactions in the Solid State. *Comprehensive Chemical Kinetics* (vol. 22). Amsterdam: Elsevier, 1980.
- [21] Jankovic B., Kolar-Anic L., Smiciklas I., Dimovic S., Arandelovic D. The nonisothermal thermogravimetric tests of animal bones combustion. Part. I. Kinetic analysis. *Thermochimica Acta* 2009;495:129–138. doi:10.1016/j.tca.2009.06.016
- [22] Ravi P., Vargeese A. A., Tewari S. P. Isoconversional kinetic analysis of decomposition of nitropyrazoles. *Thermochimica Acta* 2012;550:83–89. doi:10.1016/j.tca.2012.10.003
- [23] Vyazovkin S., Sbirrazzuoli N. Isoconversional kinetic analysis of thermally stimulated processes in polymers. *Macromol. Rapid Commun* 2006;27:1515–1532. doi:10.1002/marc.200600404
- [24] Friedmann H. L. Kinetics of thermal degradation of char-forming plastics from thermogravimetry Application to phenolic plastic. *J. Polym. Sci.* 1964;6:183–195. doi:10.1002/polc.5070060121
- [25] Ozawa T. A new method of analyzing thermogravimetric data. *Bull. Chem. Soc. Japan* 1965;38(11):1881–1886. doi:10.1246/bcsj.38.1881
- [26] Flynn J. H., Wall L. A. General treatment of the thermogravimetry of polymers. *J. Res. Nat. Bur. Standards* 1966;70A(6):487–523. doi:10.6028/jres.070A.043
- [27] Standard Test Method for Arrhenius Kinetic Constants for Thermally Unstable Materials. ANSI/ASTM E698 - 79. ASTM: Philadelphia, 1979.
- [28] Kissinger H. E. Reaction Kinetics in Differential Thermal Analysis. *Anal. Chem.* 1957;29(11):1702–1706. doi:10.1021/ac60131a045
- [29] Doyle C. D. Kinetic analysis of thermogravimetric data. *J. Appl. Polym. Sci.* 1961;5:285–292. doi:10.1002/app.1961.070051506
- [30] Sbirrazzuoli N., Vincent L., Mija A., Guigo N. Integral, differential and advanced isoconversional methods: complex mechanisms and isothermal predicted conversion-time curves. *Chemom. Intell. Lab. Syst.* 2009;96:219–226. doi:10.1016/j.chemolab.2009.02.002
- [31] Coats A. W., Redfern J. P. Kinetic parameters from thermogravimetric data. *Nature* 1964;201:68–69. doi:10.1038/201068a0
- [32] Bahng M. K., Mukarakate C., Robichaud D. J., Nimlos M. R. Current technologies for analysis of biomass thermochemical processing: a review. *Anal. Chim. Acta.* 2009;651:117–138. doi:10.1016/j.aca.2009.08.016
- [33] Dhaundiya A., Tewari P. C. Kinetic Parameters for the Thermal Decomposition of Forest Waste Using Distributed Activation Energy Model (DAEM). *Environment and Climate Technologies* 2017;19:15–32. doi:10.1515/ruect-2017-0002

- [34] Dhaundiya A., Gangwar J. Kinetics of the thermal decomposition of pine needles. *Acta Uni. Sapientiae, Agriculture and Environment* 2015:7:5–22. [doi:10.1515/ausae-2015-0001](https://doi.org/10.1515/ausae-2015-0001)
- [35] Gai C., Zhang Y., Chen W. T., Zhang P., Dong Y. Thermogravimetric and kinetic analysis of thermal decomposition characteristics of low-lipid microalgae. *Bioresour. Technol.* 2013:150:139–148. [doi:10.1016/j.biortech.2013.09.137](https://doi.org/10.1016/j.biortech.2013.09.137)
- [36] Idris S. S., Rahman N. A., Ismail K. Combustion characteristics of Malaysian oil palm biomass, sub-bituminous coal and their respective blends via thermogravimetric analysis (TGA). *Bioresour. Technol.* 2012:123:581–591. [doi:10.1016/j.biortech.2012.07.065](https://doi.org/10.1016/j.biortech.2012.07.065)
- [37] Sovizi M. R., Hajimirsadeghi S. S., Naderizadeh B. Effect of particle size on thermal decomposition of nitrocellulose. *Journal of Hazardous Materials* 2009:168:1134–1139. [doi:10.1016/j.jhazmat.2009.02.146](https://doi.org/10.1016/j.jhazmat.2009.02.146)
- [38] Vyazovkin S., Wight C. A. Model-free and model-fitting approaches to kinetic analysis of isothermal and nonisothermal data. *Thermochimica acta* 1999:340–341:53–68. [doi:10.1016/S0040-6031\(99\)00253-1](https://doi.org/10.1016/S0040-6031(99)00253-1)
- [39] Kumar A., Wang L., Dzenis Y., Jones D., Hanna M. Thermogravimetric characterization of corn stover as gasification and pyrolysis feedstock. *Biomass Bioenergy* 2008:32:460–467. [doi:10.1016/j.biombioe.2007.11.004](https://doi.org/10.1016/j.biombioe.2007.11.004)
- [40] Cai J. M., Liu R. H. Parametric study of the nonisothermal n^{th} -order distributed activation energy model involved the weibull distribution for biomass pyrolysis. *Journal of Thermal Analysis and Calorimetry* 2007:89:971–975. [doi:10.1007/s10973-006-8266-y](https://doi.org/10.1007/s10973-006-8266-y)
- [41] Dhaundiya A., Singh S. B. Parametric Study of n^{th} Order Distributed Activation Energy Model for Isothermal Pyrolysis of Forest Waste Using Gaussian Distribution. *Acta Technologica Agriculturae* 2017:20:23–28. [doi:10.1515/ata-2017-0005](https://doi.org/10.1515/ata-2017-0005)
- [42] Lim A. C. R., Chin B. L. F., Jawad Z. A., Hii K. L. Kinetic analysis of rice husk pyrolysis using Kissinger-Akahira-Sunose (KAS) method. *Procedia Engineering* 2016:148:1247–1251. [doi:10.1016/j.proeng.2016.06.486](https://doi.org/10.1016/j.proeng.2016.06.486)



Alok Dhaundiya. In 2014, He had been awarded the master's degree in mechanical engineering from GBPUAT, Uttarakhnad, India. From 2015 to 2017, he worked as an Assistant Professor in Himgiri Zee University. He has also worked on Deutsche Gesellschaft für Internationale Zusammenarbeit (GIZ) projects, which are the part of Indo-German Govt. Programme to promote renewable energy sector of India under the patronage of state government agency of Uttarakhnad, India, UREDA; and Central ministry, Ministry of New Renewable Energy. Author's area of expertise is the energy generation through the biomass waste utilization. In 2017, He received the Stipendium Hungaricum award granted by the government of Hungary. The Faculty of Engineering Excellence award has been conferred on him by the University of Strathclyde, Scotland, United Kingdom. He has also received University Grant Commission (2017 to 2022) and GATE (2012 to 2014) scholarships for his higher studies. Currently, he is the doctoral student (Mechanical) in Szent Istvan University (St. Stephen University), Hungary. ORCID: <https://orcid.org/0000-0002-3390-0860>



Prof. Suraj. B. Singh. Is a Professor in the Department of Mathematics, Statistics and Computer Science, G. B. Pant University of Agriculture and Technology, Pantnagar, India. He has 24 years of teaching and research experience with Undergraduate and Post Graduate students at different Engineering Colleges and University. Prof. Singh is a member of Indian Mathematical Society, Operations Research Society of India, ISST, and National Society for Prevention of Blindness in India and Member of Indian Science Congress Association. He is a regular reviewer of many books and International/National Journals. Mr. Singh has been a member of organizing committees in many international and national conferences and workshops. He is an Editor of the Journal of Reliability and Statistical Studies. He has authored and co-authored eight books on different courses of Applied/ Engineering Mathematics. He has won five national awards. He has published his research works at national and international journals of repute. Author's area of research is Reliability Theory.



Muammel M. Hanon is currently PhD student in Mechanical Engineering in Szent István University (Hungary) and obtained the master's degree in the field of Laser/Mechanical Engineering at University of Baghdad (Iraq) in 2011. He completed the B.Sc. degree in the field of Mechanical Engineering at the university of Technology/Baghdad in 2007. He works as a lecturer in the Middle Technical University, Iraq. He has also worked as the manager of IDs issuing department in Iraqi Engineers Union for 7 years (2007–2014). He has some publications at International journals e.g. (Experimental and theoretical investigation of the drilling of alumina ceramic using Nd:YAG pulsed laser, *Journal of Optics and Laser Technology*, <https://doi.org/10.1016/j.optlastec.2011.11.010>) and (Laser welding of copper with stellite 6 powder and investigation using LIBS technique, *Journal of Optics and Laser Technology*, <https://doi.org/10.1016/j.optlastec.2012.05.001>). The Author is a member of “Arab Engineers Union” and “Iraqi Engineers Union”. Author's research area entails laser materials processing, renewable energy and tribology of 3D printed polymers.

E-mail: Muammel_mmr_85@yahoo.com or Sharba.Muammel.M.Hanon@phd.uni-szie.hu

ORCID: <https://orcid.org/0000-0003-4811-5723>



Rekha Rawat has completed her M.Sc. with major Environmental Science from Doon University, Dehradun, Uttarakhand, India. Currently, she has been working in Himgiri Zee University, Dehradun, Uttarakhand, India. Her field of expertise is in Environmental Impact Assessment and Sustainability.